The fission yeast Stn1-Ten1 complex limits telomerase activity via its SUMO-interacting motif and promotes telomeres replication

Samah Matmati, Melina Vaurs, Jose Miguel Escandell, Laetitia Maestroni, Toru Nakamura, Miguel G. Ferreira, Vincent Geli, Stephane Coulon

▶ **To cite this version:**

Samah Matmati, Melina Vaurs, Jose Miguel Escandell, Laetitia Maestroni, Toru Nakamura, et al.. The fission yeast Stn1-Ten1 complex limits telomerase activity via its SUMO-interacting motif and promotes telomeres replication. Science Advances , 2018, 4 (5), pp.eaar2740. 10.1126/SCIADV.AAR2740 . hal-02438807

HAL Id: hal-02438807
https://hal.science/hal-02438807

Submitted on 26 Nov 2020

HAL is a multi-disciplinary open access archive for the deposit and dissemination of scientific research documents, whether they are published or not. The documents may come from teaching and research institutions in France or abroad, or from public or private research centers.

L'archive ouverte pluridisciplinaire **HAL**, est destinée au dépôt et à la diffusion de documents scientifiques de niveau recherche, publiés ou non, émanant des établissements d'enseignement et de recherche français ou étrangers, des laboratoires publics ou privés.

MOLECULAR BIOLOGY

The fission yeast Stn1-Ten1 complex limits telomerase activity via its SUMO-interacting motif and promotes telomeres replication

Samah Matmati,[1] Mélina Vaurs,[1] José M. Escandell,[2] Laetitia Maestroni,[1] Toru M. Nakamura,[3] Miguel G. Ferreira,[2,4] Vincent Géli,[1]* Stéphane Coulon[1]*

Copyright © 2018 The Authors, some rights reserved; exclusive licensee American Association for the Advancement of Science. No claim to original U.S. Government Works. Distributed under a Creative Commons Attribution NonCommercial License 4.0 (CC BY-NC).

Mammalian CST (CTC1-STN1-TEN1) complex fulfills numerous functions including rescue of the stalled replication forks and termination of telomerase action. In fission yeast lacking the CTC1 ortholog, the Stn1-Ten1 complex restricts telomerase action via its sumoylation-mediated interaction with Tpz1^{TPP1}. We identify a small ubiquitin-like modifier (SUMO)–interacting motif (SIM) in the carboxyl-terminal part of Stn1 and show that this domain is crucial for SUMO and Tpz1-SUMO interactions. Point mutations in the SIM (Stn1-226) lead to telomere elongation, impair Stn1-Ten1 recruitment to telomeres, and enhance telomerase binding, revealing that Stn1 SIM domain contributes to the inhibition of telomerase activity at chromosome ends. Our results suggest that Stn1-Ten1 promotes DNA synthesis at telomeres to limit single-strand DNA accumulation. We further demonstrate that Stn1 functions in the replication of telomeric and subtelomeric regions in a Taz1-independent manner. Genetic analysis reveals that misregulation of origin firing and/or telomerase inhibition circumvents the replication defects of the *stn1-226* mutant. Together, our results show that the Stn1-Ten1 complex has a dual function at telomeres by limiting telomerase action and promoting chromosome end replication.

INTRODUCTION

Telomeres are nucleoprotein structures that protect chromosome ends from degradation and ensure efficient replication of terminal DNA. Telomeric DNA consists of G-rich repetitive sequences, ending in a 3′ single-stranded overhang (G-tail). In mammals, the so-called shelterin complex (or telosome) is composed by telomeric repeat factor 1 (TRF1) and TRF2 that bind the telomeric double-stranded DNA, RAP1 that associates with TRF2, POT1-TPP1 that bind single-stranded DNA (ssDNA) overhang, and TIN2 that bridges the shelterin subcomplexes (*1*, *2*).

To counteract telomere attrition that occurs at each cycle of DNA replication, cells have a reverse transcriptase, the telomerase, that can add DNA to the G-tail to elongate telomeres (*2*, *3*). In humans, telomerase recruitment to telomeres is mediated by interaction between the TEN domain of telomerase catalytic subunit TERT (*4*) and the TEL patch of TPP1 (*5*, *6*). After G-tail elongation, telomerase is inhibited by the CST (CTC1-STN1-TEN1) complex (*7*, *8*), which interacts with the primase-Polα (Prim-Polα) complex for the synthesis of the complementary C-rich strand (*9*, *10*). Inhibition of telomerase is thought to be achieved by primer sequestration and also by physical interaction with POT1-TPP1 (*8*). In general, the CST also facilitates replication of telomeric DNA and other fragile sites, likely by promoting replication restart of the stalled replication forks (*11*, *12*). However, the molecular mechanism of action of CST at telomeres remains unclear (*13*).

The fission yeast *Schizosaccharomyces pombe* became an attractive model in the telomere field since the discovery of a shelterin-like structure (*14*), underscoring the evolutionary conservation of telomere composition between fission yeast and mammals. The fission yeast shelterin complex consists of Taz1 that specifically binds to duplex telomeric DNA, the G-tail–binding protein Pot1, and the four telomeric proteins Tpz1, Rap1, Poz1, and Ccq1 that link Taz1 and Pot1 through a network of protein-protein interactions (*15*, *16*). Taz1 is the homolog of TRF1-2 and interacts with Rap1. Both proteins act as a negative regulator of the telomerase (*17*), but only Taz1 facilitates semiconservative replication of telomeres (*18*). Pot1, the homolog of human POT1, associates with the G-strand overhang and binds to Tpz1, an ortholog of mammalian TPP1. Despite the lack of any obvious homology with protein of other species, Poz1 bridges the Pot1-Tpz1 to Taz1-Rap1 and may suit for the role of a TIN2 ortholog, which bridges TRF2 to POT1-TPP1 (*14*). Ccq1, which interacts with Tpz1, has no clear ortholog in other organisms; however, it performs several telomeric functions such as telomere protection and telomerase recruitment (*19*). The fission yeast telomerase complex includes the catalytic subunit Trt1^{TERT}, the regulatory subunit Est1, and the TER1^{TERC} RNA. Subsequently to Ccq1 phosphorylation by the Rad3^{ATR} kinase and telomerase recruitment (*20*, *21*), Tpz1 is sumoylated on Lys^{242} by the E3-ligase Pli1 to inhibit telomerase action, likely by recruitment of the Stn1-Ten1 complex (*22*–*24*). Stn1-Ten1 fulfills an important function in telomere protection (*25*), although the third component of CST complex, CTC1, is lacking in *S. pombe* (or has not been identified yet). The N-terminal part of Stn1 (NStn1) contains an oligonucleotide binding (OB)–fold domain that is required for interaction with Ten1, whereas its C-terminal domain displays two winged helix-turn-helix motifs (WH1-2) (*26*). WH domains are known to provide interface for substrate binding, typically DNA (*27*). *stn1* and *ten1* are both essential genes and deletion mutants eventually survive by circularizing their chromosomes, suggesting that both proteins fulfill crucial functions for telomere maintenance (*25*). More recently, a thermosensitive allele (*ts*) of *stn1* (*stn1-1*) has been isolated and characterized (*28*). At a restrictive temperature, *stn1-1* cells lose their telomeric and subtelomeric sequences, suggesting that Stn1 is also required for semiconservative replication of these regions. Despite these observations, the mechanism of action of the Stn1-Ten1 heterodimer is not fully understood.

[1]CRCM, CNRS, INSERM, Aix-Marseille Université, Institut Paoli-Calmettes, Equipe Labellisée Ligue, 27 Boulevard Lei Roure, Marseille, France. [2]Telomere and Genome Stability Laboratory, Instituto Gulbenkian de Ciência, Oeiras, Portugal. [3]Department of Biochemistry and Molecular Genetics, University of Illinois at Chicago, Chicago, IL 60607, USA. [4]Institute for Research on Cancer and Aging, Nice, Faculty of Medicine, CNRS UMR7284, INSERM U1081, University of Nice Sophia Antipolis, Nice, France.
*Corresponding author. Email: stephane.coulon@inserm.fr (S.C.); vincent.geli@inserm.fr (V.G.)

Downloaded from http://advances.sciencemag.org/ on November 26, 2020

As illustrated by the posttranslational modification of Tpz1, regulation of telomere length in fission yeast depends on SUMOylation. Deletion of *pmt3* and *pli1* genes encoding the small ubiquitin-like modifier (SUMO) peptide and the E3-ligase, respectively, cause telomere elongation (*29*, *30*). SUMO modification is often recognized by a sequence of amino acids that contains hydrophobic residues (V/I-X-V/I-V/I) plus polar/acidic residues, named SUMO-interacting motif (SIM) or SUMO-binding motif (*31*–*33*). Recent studies have shown that Stn1 interacts with SUMO (*22*, *23*), suggesting that Stn1 has a SIM domain. Here, we identified a SIM domain in Stn1 and showed that this motif is crucial for SUMO and Tpz1-SUMO interactions. Mutations in the SIM of Stn1 (*stn1-226*) cause a long-telomere phenotype. This phenotype results from a reduced recruitment of Stn1-Ten1 to telomeres and, as a consequence, retention of telomerase at telomeres. Furthermore, we uncovered an unexpected essential function of Stn1 in the replication of telomeric and subtelomeric regions. Our data also suggest that Stn1-Ten1 promotes the progression of replication fork through these regions. Together, our results indicate that the Stn1-Ten1 complex has a dual function at telomeres: First, it limits telomerase action, and second, it contributes to chromosome end replication.

RESULTS

Stn1 has a SIM domain

To understand how Stn1-Ten1 is recruited to telomeres, we analyzed Stn1-Ten1 interaction with SUMO and a chimeric protein SUMO-$Tpz1_{243-420}$ (referred to as SUMO-Tpz1) that was previously characterized in yeast two-hybrid assays (Y2H) (*23*). To this purpose, we constructed a fusion protein that mimics the Stn1-Ten1 complex. On the basis of the crystal structure of the complex that shows that Ten1 interacts with the NStn1, we engineered a protein fusion (Ten1Stn1) in which Ten1 is separated from Stn1 by a Gly^{15} amino acid linker. According to previous results, we confirmed that Ten1Stn1 displays a strong interaction with SUMO and SUMO-Tpz1 by Y2H (Fig. 1A), suggesting that the Stn1-Ten1 complex has at least one SIM domain. Because SUMO-Tpz1 was previously reported to interact with Stn1 (*22*, *23*), we inferred that Stn1 interacted with SUMO and not with Ten1. To identify the location of SIM domain in the Stn1 protein, we separately expressed the N-terminal domain containing the OB-fold domain ($NStn1_{1-156}$) and its C-terminal part ($CStn1_{157-325}$) and assessed SUMO interaction by Y2H. As expected, NStn1 strongly interacted with Ten1, in agreement with crystal structure (*26*), but no interaction was detected with SUMO (Fig. 1A). In contrast, we observed a robust interaction between CStn1 and SUMO (Fig. 1A), indicating that the CStn1 contains SIM domain(s).

Thus, we investigated the presence of the consensus SIM motif in CStn1 by sequence analysis (*33*) and found a potential hydrophobic core (^{226}ILAL^{229}) located in the first winged-helix-turn-helix motif (WH1) of Stn1 (Fig. 1B). To assess the functional significance of the putative SIM, we substituted leucine and isoleucine amino acids in this motif by alanine (SIM ^{226}AAAA^{229}). Replacements of these hydrophobic residues by alanine are known to reduce SIM/SUMO interaction (*31*). These modifications of the SIM in CStn1 abolished the interaction with SUMO and SUMO-Tpz1 in the Y2H assay (Fig. 1C).

Next, we introduced SIM point mutations into chromosomally encoded Stn1 using a pop-in/pop-out strategy. We generated a *stn1-SIM* strain, referred to as *stn1-226* mutant. This *stn1-226* mutant was spotted on yeast exract base medium (YES) and YES-phloxine plates at 25°, 32°, and 36°C (Fig. 1D). We observed that point mutations in SIM caused growth defects at 36°C. At this temperature, cells displayed a dark pink color in the presence of phloxine, which reflects cell sickness. At 32°C, cell growth was not affected; however, dark pink–colored colonies were visible. Growth retardation was detected 12 hours after temperature shift to 36°C (Fig. 1D). Therefore, the *stn1-226* allele behaved as a *ts* mutant. Telomere length analysis at 25°C showed that SIM point mutations caused a significant telomere elongation phenotype (Fig. 1E). The length of telomeric repeated sequences was estimated at an average of 915 base pairs (bp) (SD = 37) in *stn1-226*, more than two times of that in the wild-type (WT) strain [403 bp (SD = 61)]. We also noticed that addition of a 13-myc tag to the C terminus of Stn1 increased telomere length in both WT and *stn1-226* strains by about the same increment (Fig. 1E). Together, these results indicate that the impediment of SUMO recognition by Stn1 provokes telomere elongation and suggest that the SIM domain of Stn1 is implicated in the recognition of the sumoylated form of Tpz1.

We also investigated the CStn1/SUMO and CStn1/SUMO-Tpz1 interactions for two additional modifications in Stn1, namely, of the ^{195}LIYL^{198}, another potential hydrophobic core of a SIM domain that was mutated to ^{195}AAYA^{198} (Stn1-195) and of the $L^{177}M$-$M^{180}I$ mutations, which corresponds to the *stn1-1* allele (Fig. 1B and fig. S1A) (*28*). *stn1-1* is a *ts* allele and displays a long-telomere phenotype comparable to the *stn1-226* strain. Unlike the Stn1-226, which completely abolished the interaction of CStn1 with SUMO and SUMO-Tpz1, these two additional modifications retained the SUMO-binding capacity (fig. S1, B and C).

To verify the function of the putative SIMs in vivo, we generated heterozygous diploid *stn1*$^{+}$*/stn1-195–myc* and *stn1*$^{+}$*/stn1-226–myc* strains, sporulated them, and analyzed the spore colonies bearing the *stn1-195* and *stn1-226* alleles. The *stn1-195–myc* mutant displayed normal growth and WT telomere length, whereas a growth defect at 36°C and elongated telomeres were observed in the *stn1-226–myc* mutant (fig. S1, D to F), phenocopying the *stn1-1* mutant (*28*). Thus, the Stn1-1 protein retained SUMO interaction, although *stn1-1* cells had long telomeres similar to those in *stn1-226* cells. We also inferred that the ^{195}LIYL^{198} motif does not function as a strict SIM domain in contrast to the ^{226}ILAL^{229} motif (Stn1-226). Curiously, the Stn1-75 protein that also carries a mutation in the ^{195}LIYL^{198} hydrophobic core of Stn1 (L198S) conferred a *ts* phenotype (*23*). This apparent discrepancy observed between the *stn1-195–myc* and *stn1-75* alleles might be explained by the fact that the hydrophobic amino acid L198 was replaced by a polar residue (serine) in the *stn1-75* protein. Notably, we were unable to generate the *stn1-195-226–myc* strain, suggesting that both mutations cause cell lethality. These results prompted us to investigate the effect of Stn1 SIM mutations (*stn1-226*) in telomere length regulation.

Stn1 interaction with Tpz1 is lost in *stn1-226* cells

To rule out the possibility that the Stn1-226 mutations affected the interaction between Stn1 and Ten1, we monitored Stn1/Ten1 interaction in WT *stn1*$^{+}$ and *stn1-226* cells at permissive and restrictive temperatures. Pulldown of Ten1-Flag was performed, and co-IP of Stn1-myc was analyzed. An interaction between Stn1-myc and Ten1-Flag was detected in both WT and *stn1-226* cells at both temperatures, although expression level of Ten1-Flag was lower at 25°C than at 36°C (Fig. 1F). This interaction was confirmed by Y2H (Fig. 1G). Similarly, we monitored the interaction between the Stn1-Ten1 complex and Tpz1 using the Ten1Stn1 fusion in the Y2H assay (Fig. 1H). We observed that Ten1Stn1-226 no longer interacted either with SUMO-Tpz1 or with SUMO, although these interactions were robust with the nonmutated

Downloaded from http://advances.sciencemag.org/ on November 26, 2020

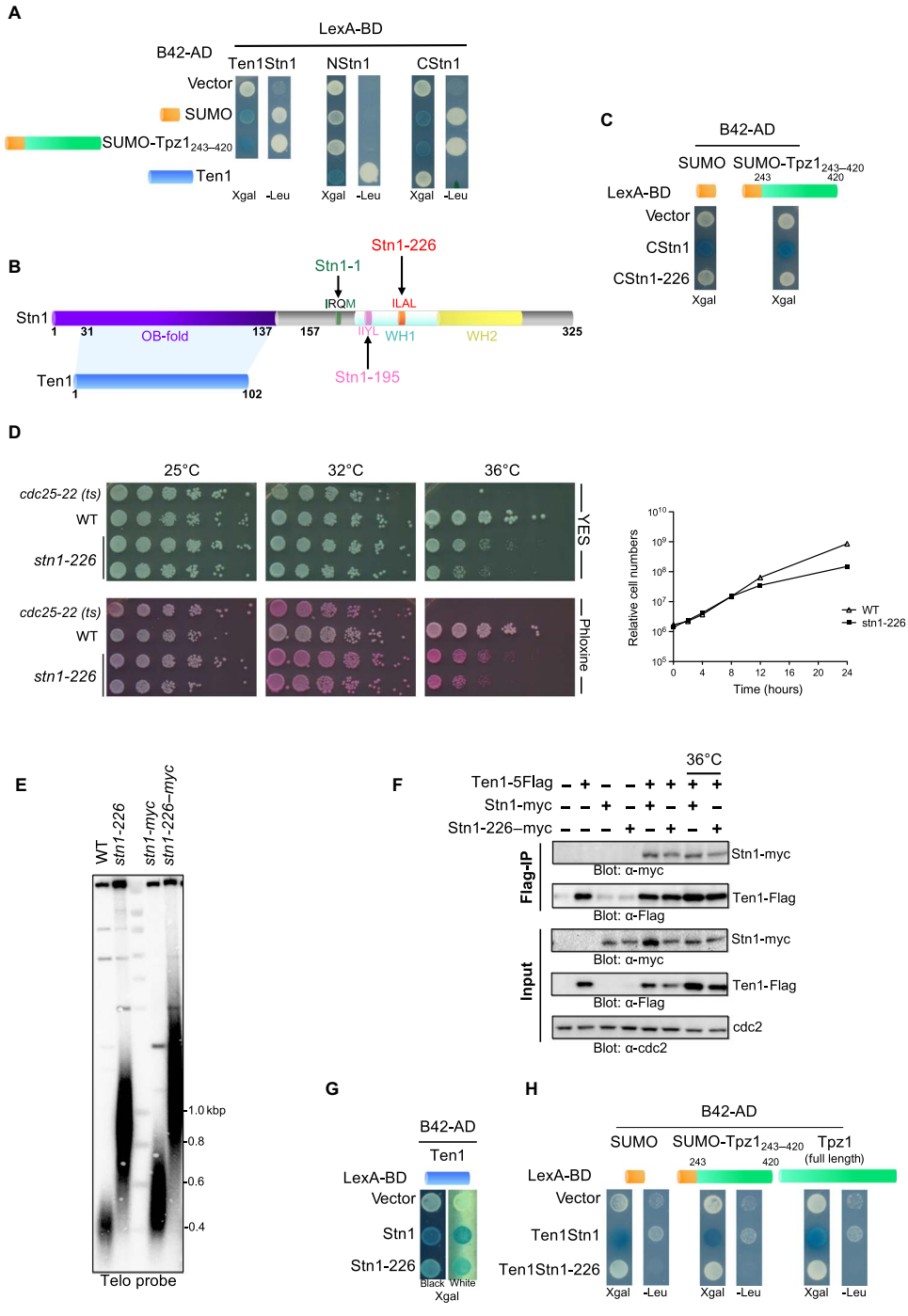

Fig. 1. Mutations of the Stn1 SIM domain lead to elongated telomeres. (**A** and **C**) Y2H analysis of budding yeast strain carrying the indicated plasmids. The indicated proteins were fused either to B42 activating domain (B42-AD) or to LexA DNA binding domain. Cells were grown and spotted on selective medium (-TRP and -HIS) to select the two Y2H plasmids and tested for the activation of either *Leu2* or *LacZ* reporters. (**B**) Schematic representation of the Stn1 and Ten1 proteins. The NStn1 contains the OB-fold domain that interacts with Ten1, whereas the CStn1 contains the WH1-2. The SIM domain that starts at position 226 is embedded into the WH1. The IRQM and the IIYL motifs mutated in the *stn1-1* and *stn1-195* alleles are also represented, respectively. (**D**) Analysis of viability of the indicated strains at different temperatures. Left: Cells were grown at 25°C, then serially diluted (fivefold), and plated on YES-rich medium either complemented or not with phloxine. Pink color reflects impaired growth. The *stn1-226* allele carries mutations in SIM (^{226}ILAL^{229} to ^{226}AAAA^{229}). Right: Growth curve of WT and *stn1-226* strains. Both strains were cultured at 25°C in YES medium and then shifted to 36°C for 24 hours. (**E**) Genomic DNA from cells with the indicated genotype was prepared, digested with Apa I, and analyzed by Southern blotting with a radiolabeled telomeric DNA probe. (**F**) Stn1/Ten1 interaction is analyzed by coimmunoprecipitation (co-IP). Pulldown was carried out using anti-Flag (M2, mouse monoclonal antibody) from cell extracts prepared from indicated cultures carried out at 25°C if not specified. The co-IP of Stn1 was monitored using anti-myc (9E10, mouse monoclonal antibody). (**G**) Ten1-Stn1 interaction analyzed by Y2H. Cells were grown and spotted on selective medium (-TRP and -HIS) and tested for activation of *LacZ* reporter. Image is displayed on black and white background to visualize the blue color. (**H**) Ten1Stn1 interactions with SUMO, SUMO-Tpz1, and Tpz1 analyzed by Y2H. Cells were grown and spotted on selective medium (-TRP and -HIS) and tested for activation of *Leu2* and/or *LacZ* reporters.

Downloaded from http://advances.sciencemag.org/ on November 26, 2020

form of Ten1Stn1 fusion. Notably, the interaction between Ten1Stn1-226 and Tpz1 was also impaired, suggesting that SIM and/or CStn1 is involved in Tpz1/Ten1Stn1 recognition regardless of Tpz1 SUMOylation status. Overall, these results showed that mutations in the SIM domain of Stn1 retained the interaction with Ten1 but lost the interaction with Tpz1. Notably, we could not manage to set up robust and convincing pulldown assays of Tpz1-Flag and Stn1-myc or Stn1-226–myc, suggesting that Stn1 transiently interacts with Tpz1.

Stn1 SIM domain is important for telomerase inhibition

Because Tpz1 SUMOylation is thought to promote Stn1-Ten1 recruitment and to limit telomerase action (*22*, *23*), we reasoned that the lengthening of telomeres in *stn1-226* mutant might result from Stn1-Ten1 recruitment defect at telomeres. Thus, we analyzed by chromatin-immunoprecipitation (ChIP) the binding of Stn1, Ten1, and Est1 in WT $stn1^{+}$ and *stn1-226* asynchronous cells at telomeres. The recruitment of Stn1-226 at telomeres was significantly reduced compared to WT Stn1 (Fig. 2A). The SIM mutation did not completely abolish Stn1 recruitment because a small fraction of Stn1-myc was still associated with telomeres in *stn1-226* cells. Consistent with these results, Ten1-Flag binding to telomere was decreased to the same level in the *stn1-226* mutant (Fig. 2A). In marked contrast to what was observed for Stn1 and Ten1, the binding of Est1 at telomeres was significantly increased in the *stn1-226* mutant (Fig. 2A). Increased Est1 recruitment was in agreement with the elongated telomere phenotype of the *stn1-226* mutant. These results indicated that the Stn1 SIM domain promotes the recruitment of Stn1-Ten1 to telomeres at the expense of telomerase binding. This also suggests that Stn1-Ten1 is recruited at a basal level to telomeres either through a SUMO-independent Tpz1 interaction or perhaps through a direct binding to ssDNA.

$tpz1^{K242R}$ *stn1-226* double mutant survives with circular chromosomes

To further investigate the role of Stn1-Ten1 in telomere length regulation, we used the nonsumoylatable form of Tpz1 mutant ($tpz1^{K242R}$ allele) (*22*, *23*). Because both $tpz1^{K242R}$ and *stn1-226* mutants displayed long telomeres, we asked whether these mutations are epistatic. Tetrad dissection analysis revealed that the spores bearing both $tpz1^{K242R}$ and *stn1-226* mutations grew at a slower rate than the corresponding single mutants (Fig. 2B). Further investigation of their telomere status by Southern blotting revealed the absence of telomeric signal in the $tpz1^{K242R}$ *stn1-226* double mutant (Fig. 2B). To test whether $tpz1^{K242R}$ *stn1-226* cells have circular chromosomes (*34*, *35*), we performed pulsed-field gel electrophoresis (PFGE) analysis of genomic DNA. As shown in Fig. 2C, the entire chromosomes of $tpz1^{K242R}$ *stn1-226* cells did not enter the gel. Further PFGE and Southern hybridization analysis of the Not I–digested genomic DNA samples with the C-I-M-L probes (Fig. 2C) showed the characteristic pattern of circularized chromosomes (*35*), thereby confirming that $tpz1^{K242R}$ *stn1-226* cells survived by circularization of their chromosomes. Thus, the combination of $tpz1^{K242R}$ and *stn1-226* alleles leads to complete loss of telomeres, mimicking, to some extent, the phenotype of the *stn1*Δ mutant (*25*). This prompted us to investigate the impact of K242R on Ten1Stn1-Tpz1 interaction using Y2H and β-galactosidase activity measurement. As previously shown in Fig. 1H, the SIM226 mutation abrogated the interaction of Ten1Stn1 with Tpz1, whereas the K242R only reduced Ten1Stn1-Tpz1 interaction (from 7 to 3 or 5 β-galactosidase U) (Fig. 2D), confirming published results (*22*). By comparison, the strength of interaction between Ten1Stn1 and SUMO or SUMO-Tpz1, measured under the same conditions, is six- to sevenfold higher than the one of Ten1Stn1 with Tpz1 (around 50 β-galactosidase U). Together, these results show that mutations in the SIM domain of Stn1, besides abrogating the Stn1 recognition of SUMO-Tpz1, fully abolish the interaction between Ten1Stn1 and Tpz1. The β-galactosidase assay did not allow determination of whether the K242R mutation exacerbated the defect of the SIM226 mutation on the Ten1Stn1-Tpz1 interaction. However, it showed that the Tpz1-K242R mutation by itself affected Tpz1 interaction with Ten1Stn1. These observations unveil a fine regulation of Stn1-Ten1 recruitment at telomeres that relies mainly on SUMO-SIM recognition but also on a direct interaction with Tpz1. These observations might explain why the $tpz1^{K242R}$ *stn1-226* mutant, in which Stn1-Ten1 recruitment at telomeres is likely fully impaired, exhibits a *stn1*Δ- and *ten1*Δ-like phenotype (*25*).

Stn1 sustains telomeric and subtelomeric DNA replication

To gain insight into the Stn1 functions, we took advantage of the *ts* phenotype of the *stn1-226* mutant and monitored telomere stability by Southern blotting after a temperature shift to 36°C (Fig. 3A). The telomeric signal rapidly decreased, whereas it remained constant in the WT strain. The membrane was stripped and rehybridized with a subtelomeric probe (STE1) (Fig. 3B). Surprisingly, the subtelomeric signal also faded at a restrictive temperature in *stn1-226* but later than the telomeric signal, as it has been described for the *stn1-1* allele (*28*). These observations indicated that the Stn1 SIM domain plays a crucial function in the replication of the telomeric and subtelomeric regions.

Because collapsed forks are often rescued by a homologous recombination pathway, we combined the *stn1-226* allele with *rad51*Δ mutant. The double mutant grew at a slower rate than each single mutant even at 25°C, indicating that Rad51 is required in *stn1-226* cells even at a permissive temperature (Fig. 3C). We therefore analyzed telomere length at 25°C in the double *rad51*Δ *stn1-226* strain (Fig. 3D). Strikingly, *stn1-226* cells lacking Rad51 exhibited a partial loss of their telomeric and subtelomeric sequences even at 25°C, comparable to *stn1-226* at a restrictive temperature. PFGE experiments further showed that *rad51*Δ *stn1-226* cells exhibit rearranged and partially circularized chromosomes (Fig. 3E), thereby confirming that *stn1-226* requires a fully functional Rad51-dependant pathway. At a high temperature, the *rad51* deletion exacerbated the synthetic sickness of the *rad51*Δ *stn1-226* cells (Fig. 3F). Overall, these observations indicated that replication stress in the *stn1-226* mutant, even at a permissive temperature, requires a functional Rad51 to maintain the telomeric and subtelomeric regions.

To better understand the nature of the DNA replication defect in the *stn1-226* mutant, we investigated replication intermediates by two-dimensional gel electrophoresis (2D-gel) at telomeres, as previously described (*18*, *36*). Genomic DNA samples from the parental WT and *stn1-226* cells, grown at permissive and restrictive temperatures, were analyzed after Nsi I digestion by Southern blotting with a subtelomeric STE1 probe. In the first dimension, we observed four distinct bands for the parental WT, but only one thick and smeared band was detected in the *stn1-226* mutant (Fig. 4A). Accordingly, Y structures that correspond to the unidirectional moving of the replication forks within the Nsi I fragment were visualized in the WT strain at both temperatures, whereas these structures were not detected in *stn1-226* cells (Fig. 4B). Replication of telomeric regions seemed to be severely affected in *stn1-226* at 25°C, leading to superimposed Y arcs mimicking, to some extent, the *taz1*Δ phenotype (*18*). At a restrictive temperature, the replication intermediates were not detected, in agreement with the disappearance of telomeric and subtelomeric sequences. Genomic DNA samples were also digested with Bam HI and analyzed by Southern blotting using a probe specific for the replication fork barrier at ribosomal DNA

Downloaded from http://advances.sciencemag.org/ on November 26, 2020

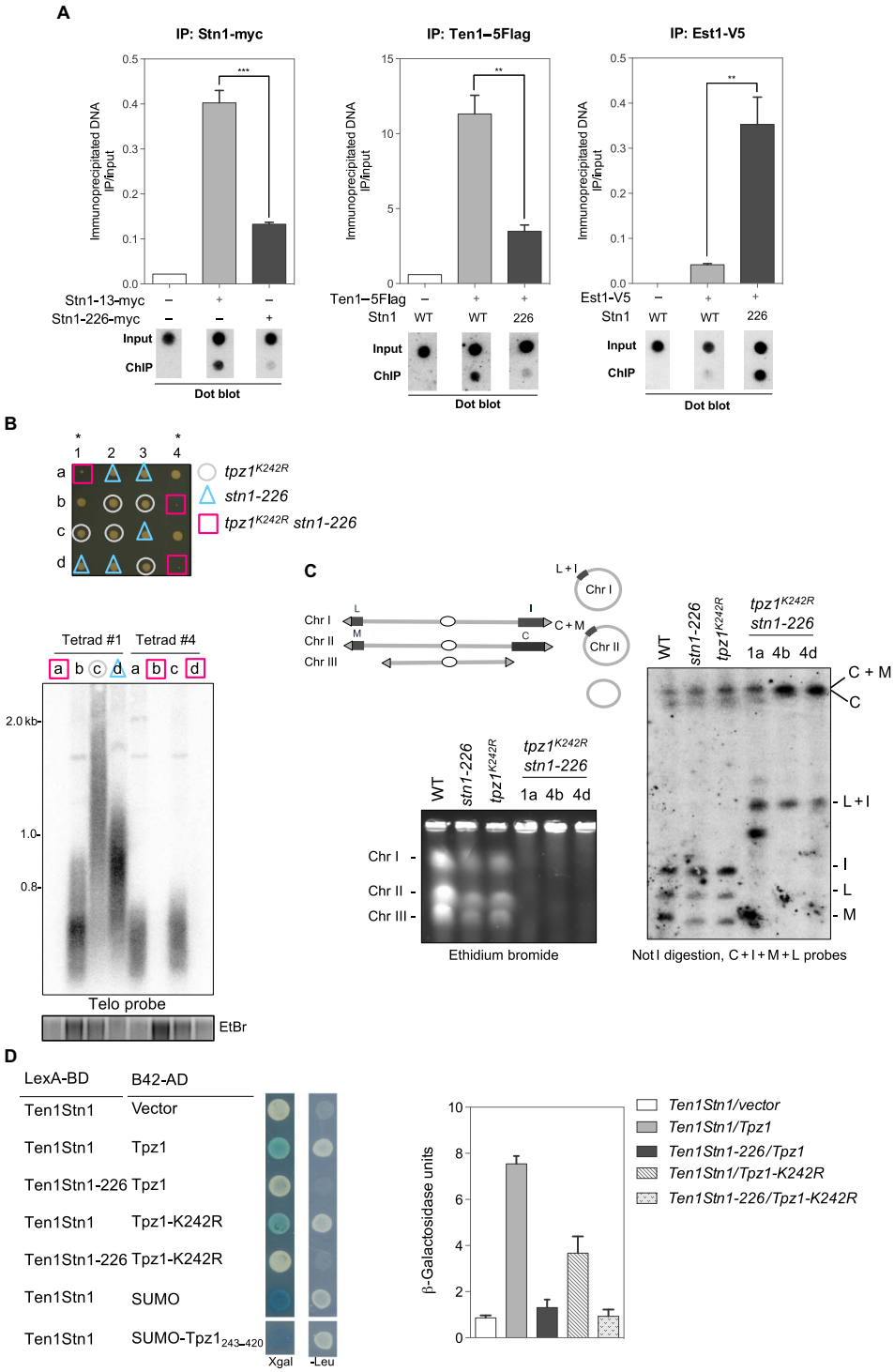

Fig. 2. Stn1 SIM mutations affect Stn1-Ten1 recruitment and enhance telomerase binding to telomeres. (**A**) Telomere association of Stn1, Ten1, and Est1 monitored with dot blot ChIP assays. ChIP experiments were performed using samples collected from 25°C exponentially growing WT *stn1*$^{+}$ and *stn1-226* cells carrying the indicated epitope-tagged proteins. Error bars indicate the SEM from multiple independent experiments ($n = 3$); P values are calculated from two-tailed t test (**$P < 0.01$ and ***$P < 0.005$). (**B**) Top: Growth of spores carrying the indicated genotypes. Bottom: Telomere length analysis of two tetrads by Southern blotting with a radiolabeled telomeric DNA probe. Genomic DNA was digested with Apa I restriction enzyme. (**C**) Left: PFGE stained by ethidium bromide (EtBr) of intact chromosomes from WT strain, parental *tpz1*^{K242R} and *stn1-226* single mutants, and *tpz1*^{K242R} *stn1-226* double mutants grown at 25°C. Chromosomes I, II, and III were stable in single mutants, whereas they did not enter into the gel in double mutants. Right: Not I–digested genomic DNA was subjected to PFGE, transferred to nitrocellulose membrane, and hybridized with probes of telomere proximal fragments C, I, M, and L. In *tpz1*^{K242R} *stn1-226* double mutants, these fragments were absent and have been replaced by DNA fragments C + M and L + I. This modification in the Not I–digested pattern is characteristic of chromosome circularization. (**D**) Ten1Stn1 interactions with Tpz1 analyzed by Y2H in different mutants. Cells were grown and spotted on selective medium (-TRP and -HIS) and tested for activation of *Leu2* and/or *LacZ* reporters. Y2H interaction was quantified by measurement of β-galactosidase activity.

Downloaded from http://advances.sciencemag.org/ on November 26, 2020

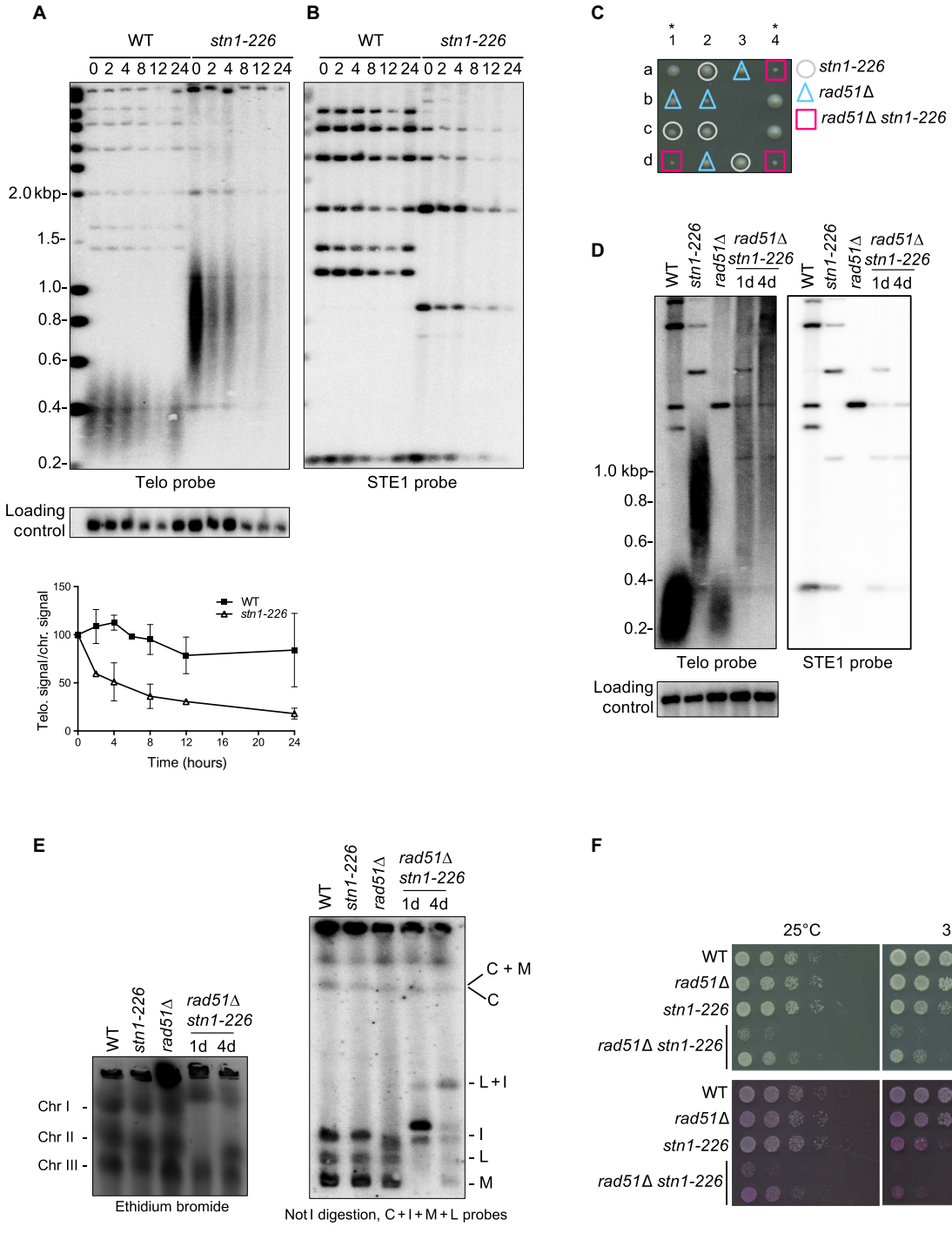

Fig. 3. Telomeric and subtelomeric regions are lost in *stn1-226* at a high temperature. (**A** and **B**) WT and *stn1-226* strains were cultivated at 25°C in YES medium and then shifted at 36°C for 24 hours. Genomic DNA was prepared, digested with Apa I restriction enzyme, and analyzed by Southern blotting with radiolabeled probes, telomeric probe (A), subtelomeric STE1 probe (B), and a chromosomic probe (used as a loading control). Quantification of normalized telomeric signal over chromosomic signal is shown in the lower panel. Error bars indicate the average from two independent experiments. At a restrictive temperature, both telomeric and subtelomeric signals disappeared in *stn1-226*. (**C**) Synthetic sickness of *rad51*Δ and *stn1-226* alleles. Spore colonies, resulting from tetrad dissection of a mating between *rad51*Δ and *stn1-226* mutants, were grown at 25°C. (**D**) Telomere length analysis of indicated strains grown at 25°C. Genomic DNA was prepared, digested with Apa I restriction enzyme, and analyzed by Southern blotting with radiolabeled telomeric, subtelomeric (STE1), and chromosomic probes (loading control). At a permissive temperature, the telomeric and subtelomeric signal disappeared in both *rad51*Δ *stn1-226* double mutants. (**E**) Left: PFGE stained by ethidium bromide of intact chromosomes from WT strain, *stn1-226*, *rad51*Δ, and *stn1-226 rad51*Δ mutants grown at 25°C. Chromosomes I, II, and III entered into the gel. Right: Not I–digested genomic DNA was subjected to PFGE, transferred to nitrocellulose membrane, and hybridized with probes of telomere proximal fragments C, I, M, and L. The *rad51*Δ *stn1-226* 4D clone exhibited a partial circularization of its chromosomes, whereas clone 1D displayed a rearranged profile with partial circularization. (**F**) Analysis of viability of the indicated strains at 25° and 36°C. Cells were grown at 25°C, then serially diluted, and plated on YES-rich medium either complemented or not with phloxine.

Downloaded from http://advances.sciencemag.org/ on November 26, 2020

(rDNA) (rDNA-RFB probe) (Fig. 4C). This allowed us to control the quality of the 2D-gel samples and also to visualize replication intermediates at a locus that is difficult to replicate, similar to telomeres. Pausing of replication forks at the RFB site causes the accumulation of identical Y structures visible as three distinct spots (RFB1-3) on the Y arc (*37*, *38*). X-shaped DNA structures are thought to arise either from converged forks or from recombination associated with DNA replication. Indistinctly, similar Y-arc and X-spike DNA structures were detected in both WT and *stn1-226* at either 25° or 36°C (Fig. 4C). Thus, we concluded that Stn1 is involved in the replication of telomeric and subtelomeric regions but not of the rDNA locus.

Stn1 functions in telomeric DNA replication in parallel to Taz1

Many obstacles challenge the replication fork progression at telomeres, and some telomere-associated proteins are known to play an important role in promoting efficient replication (*39*). In fission yeast, Taz1 and the replication protein A (RPA) complex are directly involved in telomere replication but act in two distinct pathways. Taz1 protein promotes replication fork progression through telomeric repeats (*16*, *18*), whereas RPA prevents G-rich DNA structures formation, including G-quadruplexes, at lagging-strand telomeres (*36*). Distinctly, Rif1 is globally involved in the temporal control of DNA replication (*40*, *41*). Thus, we analyzed the genetic interaction between *stn1-226* and *rpa1-D223Y* and *taz1*Δ and *rif1*Δ mutants. Analysis of tetrad dissections and spot assays showed that *rpa1-D223Y* and *stn1-226* did not exhibit any genetic interaction at either 25° or 36°C (Fig. 5A). Southern blot analysis revealed that the *stn1-226 rpa1-D223Y* double mutant has telomeres of an intermediate size between the short telomeres of *rpa1-D223Y* and the long ones of *stn1-226* (Fig. 5A). One interpretation would be that loss of telomerase regulation in *stn1-226* cells compensates the telomere shortening caused by the G-quadruplex unwinding defect in the *rpa1-D223Y* mutant. In contrast, deletion of $taz1^{+}$ exacerbated the *ts* phenotype when combined with the *stn1-226* allele at a restrictive temperature (Fig. 5B). Surprisingly, telomeres were totally lost in *stn1-226 taz1*Δ cells at a permissive temperature (Fig. 5B). PFGE analysis showed that *taz1*Δ *stn1-226* chromosomes did not enter into the gel (Fig. 5C). Further Southern hybridization analysis of Not I–digested genomic DNA revealed that double mutant did not exhibit the classical C-I-M-L pattern of linear chromosomes, suggesting that *stn1-226 taz1*Δ cells underwent catastrophic chromosome rearrangements. We could not distinguish L + I fragments in *stn1-226 taz1*Δ cells, indicating that double mutants may not survive by circularizing their chromosomes but rather have linear HAATI-like chromosomes (*42*). The *stn1-226 taz1*Δ did not display a growth defect at 25°C, although it loses telomeric sequences as does the $tpz1^{K242R}$ *stn1-226* double mutant that displays circular chromosomes (Fig. 2C). This might suggest that chromosome rearrangements occur differently in the *stn1-226 taz1*Δ cells.

In contrast, when the *stn1-226* allele was combined with $rif1^{+}$ deletion, we observed a complete rescue of the *ts* phenotype of the *stn1-226* mutant (Fig. 5D), similar to what has been previously observed in the *stn1-1* cells (*28*). Telomere length analysis showed that *stn1-226 rif1*Δ harbored very long telomeres in comparison to each single mutant, showing that the control of telomere length by Stn1 and Rif1 is independent. Rif1 is a multifaceted protein that is involved in yeast in telomerase inhibition (*17*, *43*), cytokinesis (*44*), and, as mentioned above, in the timing of the replication (*40*, *41*). These functions depend on Rif1 association with PP1 phosphatases (Dis2 and Sds21 in fission yeast) (*44*, *45*). To test whether the rescue of *stn1-226* phenotypes by *rif1*Δ is phenocopied by the *rif1-PP1* allele, we combined *stn1-226* with *rif1-PP1*. We observed that *rif1-PP1* suppresses the *ts* phenotype of *stn1-226* but to a lesser extent than *rif1*Δ (Fig. 5D). This observation is in agreement with the result of Takikawa *et al.* (*28*), who identified *dis2* and *sds21* deletions as suppressors of the *stn1-1 ts* phenotype. Thus, the suppression of Stn1-226 defects by *rif1* deletion is partially mediated by PP1 phosphatases.

We further constructed a *stn1-226 rap1*Δ double mutant. Rap1 shares with Rif1 the negative regulation of telomerase (*17*, *18*). We found that *rap1*Δ partially suppresses the *stn1-226 ts* phenotype (Fig. 5E), suggesting that the release of telomerase inhibition in *rap1*Δ and *rif1*Δ also participates to the suppression of *stn1-226* phenotypes at a restrictive temperature. Because *taz1*Δ also alleviates telomerase inhibition, it also suggests that the synergic effect observed in *taz1*Δ *stn1-226* is caused by a defect of replication fork progression at telomeres. Collectively, these observations indicate that origin firing and high activity of telomerase both possibly circumvent the impediment of telomere replication at a high temperature caused by mutation in the SIM domain of Stn1. We also cannot rule out the fact that telomere replication defect of Stn1-226 provokes telomere entanglements at anaphase and that the deletion of $rif1^{+}$ suppresses potential cytokinesis defect of *stn1-226* cells, as it does in *taz1*Δ (*17*).

Overexpression of catalytic subunit of Polα rescues *stn1-226*

As shown above, our results indicate that Stn1 promotes DNA replication at telomeres and subtelomeres. Although we could not detect significant impediment of replication at rDNA, we asked whether Stn1 is required when replication is challenged by DNA-damaging agents. The *stn1-226* mutant was spotted on YES plates in the presence of camptothecin, methyl methanesulfonate, and hydroxyurea (Fig. 6A). We observed that the *stn1-226* mutant exhibited sensitivity to all three drugs, a phenotype that is suppressed by the *rif1* deletion (fig. S2A). These results indicate that Stn1 is required when replication forks are slowed down or stalled after DNA damage, likely to promote DNA synthesis or fork restart. To test this hypothesis, we overexpressed the catalytic subunit of the DNA polymerase α (Pol1) from the pREP41-Pol1 plasmid in *stn1-226* cells. We observed that Pol1 overexpression slightly rescued the *ts* phenotype of *stn1-226* (Fig. 6B). To confirm this effect, we measured the plating efficiency of *stn1-226*–overexpressing Pol1. Figure 6C shows the ratio of colony-forming units (CFU) at 32° and 36°C over the CFU at 25°C. Plating efficiency at 32° and 36°C was reduced to 54 and 20% in *stn1-226* cells, respectively. When Pol1 was expressed, plating efficiency at 36°C increased up to 38%. This confirmed that Pol1 overexpression is able to partially rescue the thermosensitivity of *stn1-226*. Next, we asked whether overexpression of Pol1 is also capable of preventing the loss of telomeric sequences at a restrictive temperature. *stn1-226* and WT cells were grown at 25°C and shifted up to 36°C for 24 hours. Teloblot analysis revealed that the presence of ectopically expressed Pol1 limits the loss telomeric signal (Fig. 6D). Quantification of several independent experiments showed that the complementation was significant, although it was only partial (likely because of the lack of the primase complex), suggesting that Stn1-Ten1 is required to reinitiate DNA synthesis at stalled or collapsed replication forks.

stn1-226 accumulates telomeric ssDNA at permissive and restrictive temperatures

This study reveals that Stn1 has two functions at telomeres: It limits telomerase action and promotes chromosome end replication. If the

Downloaded from http://advances.sciencemag.org/ on November 26, 2020

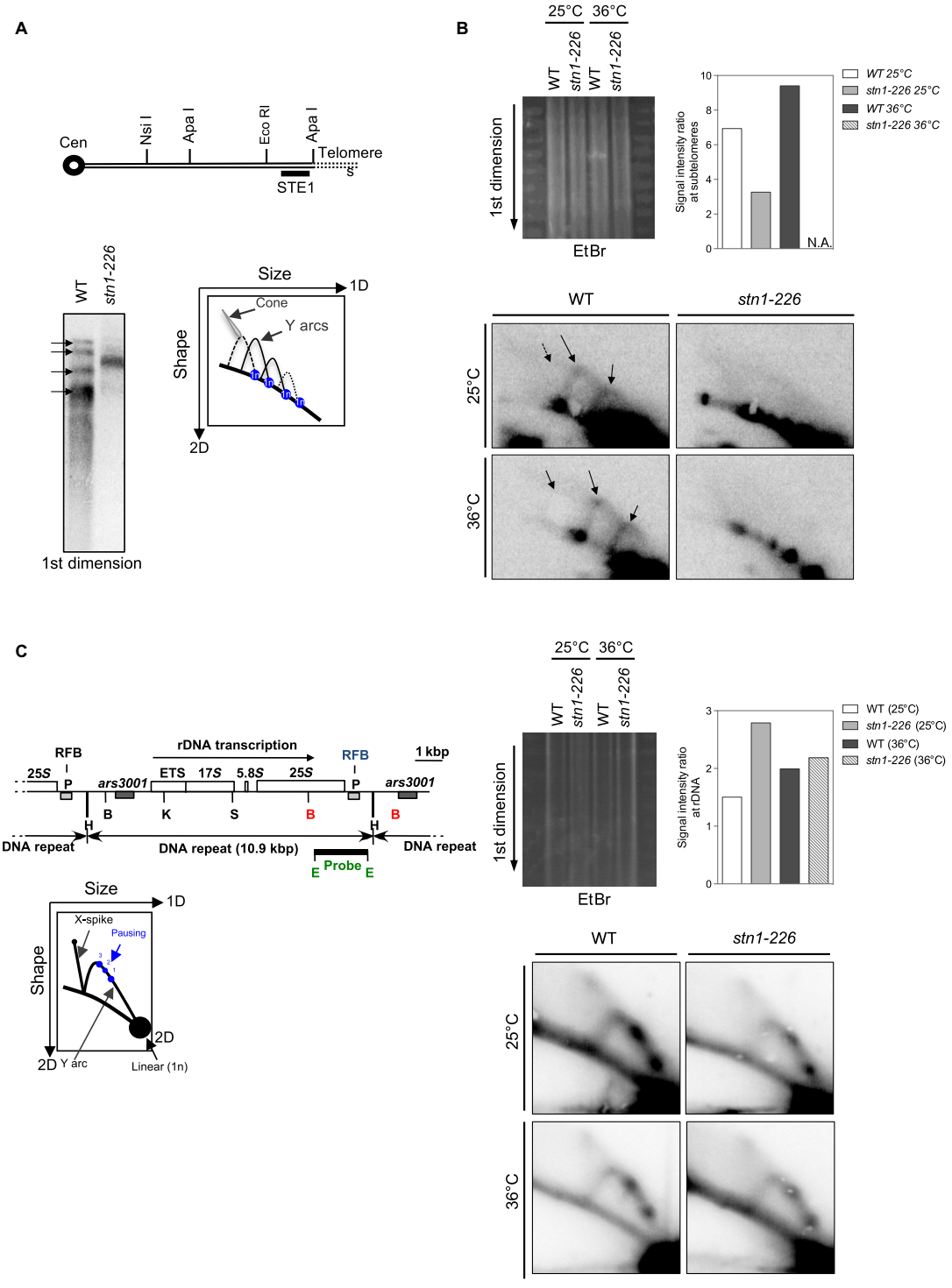

Fig. 4. Stn1 is required to promote efficient replication of telomeric regions. (**A**) Relative position of the restriction sites in the subtelomeric regions of chromosomes I and II. The subtelomeric probe (STE1) that is used for 2D-gel hybridization (see below) is represented. Cen, centromere. Southern blot analysis of Nsi I telomeric fragments (first dimension) from the parental WT strain and *stn1-226* mutant revealed by STE1 probe. (**B**) 2D-gel analysis of Nsi I telomeric fragments of WT and *stn1-226* strains at 25°C and after 24 hours at 36°C. The first dimension of the EtBr-stained gel was photographed before the second dimension. The Y-arc pattern is generated by unidirectional movement of a replication fork across each telomeric fragment shown in the first dimension. The cone-shaped signal represents four-way DNA junctions (double Y). Quantification of the total replication intermediate signal over the linear arc signal of rDNA is presented. N.A., not available. (**C**) Top: Map of the rDNA repeats. Boxes indicate the *ars3001* and the RFB pause sites (P). The restriction enzyme sites are indicated (H, Hind III; B, Bam HI; K, Kpn I; S, Sac I; E, Eco RI). Left: Diagram of the migration pattern of replication intermediates that can be detected by 2D-gel electrophoresis. Right: 2D-gel analysis of rDNA RFB site in WT and *stn1-226* strains at permissive and restrictive temperatures. The first dimension of the EtBr-stained gel was photographed before the second dimension. Quantification of the total replication intermediate signal over the linear arc signal is presented. The Eco RI–Eco RI fragment is used as a probe.

Downloaded from http://advances.sciencemag.org/ on November 26, 2020

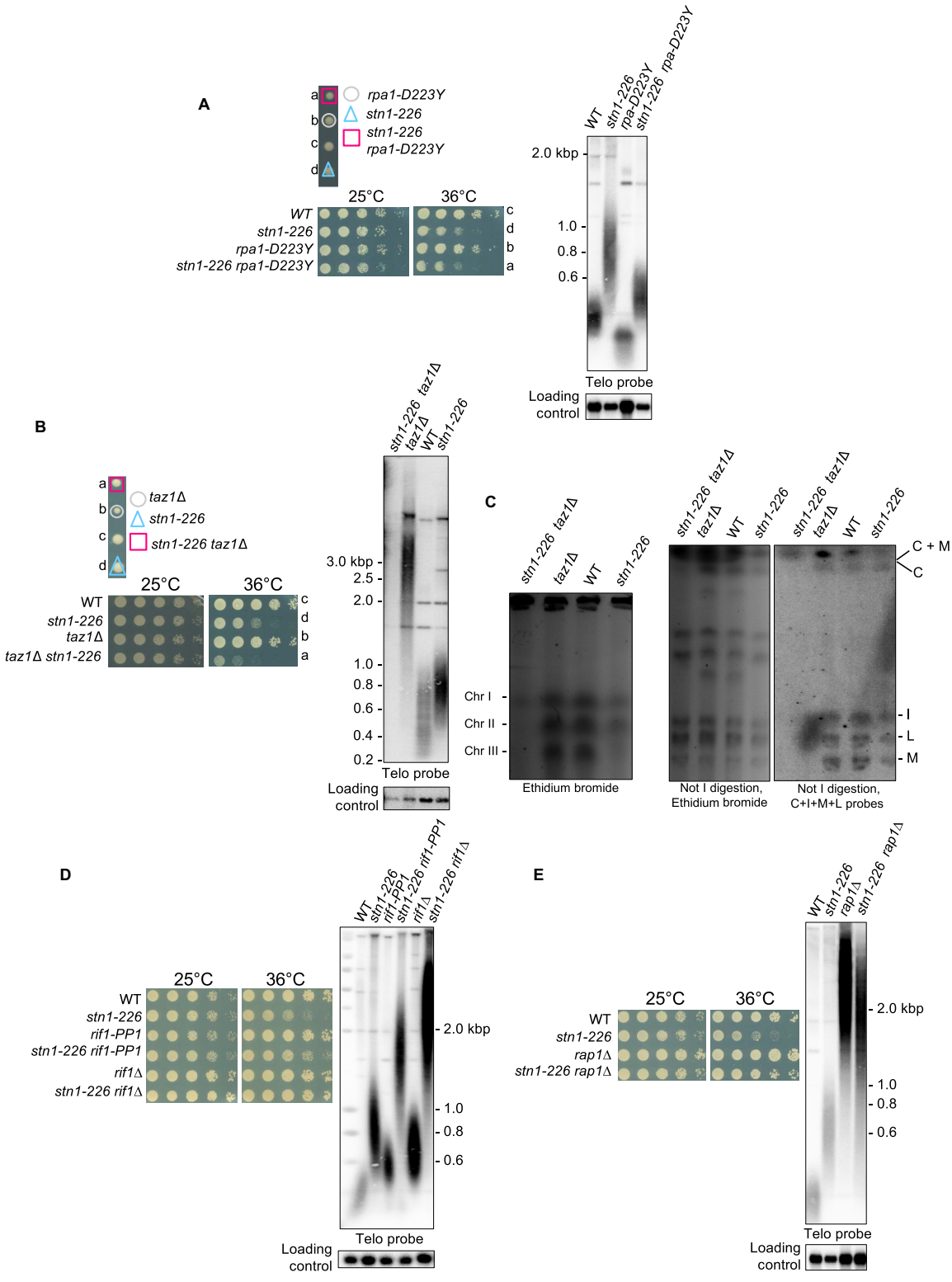

Fig. 5. Genetic interactions of *stn1-226* allele with *rpa1-D223Y*, *taz1*Δ, *rif1*Δ, *rif1-PP1*, and *rap1*Δ. (**A** to **E**) Tetrad dissections, telomere length analysis, and viability of the indicated spore colonies are shown. Analysis of viability was carried out at 25° and 36°C. Cells were grown at 25°C, then serially diluted (fivefold), and plated on YES-rich medium. Cells were grown at 25°C, and genomic DNA was digested with Apa I restriction enzyme for telomere Southern blotting analysis. Loading control corresponds to a 2.4-kbp fragment of a chromosomic region. (**C**) Left: PFGE stained by ethidium bromide of intact chromosomes from WT strain, parental *taz1*Δ and *stn1-226* single mutants, and *taz1*Δ *stn1-226* double mutants. Chromosomes I, II, and III were stable in single mutants, whereas they did not enter into the gel in double mutants. Right: Not I–digested genomic DNA was subjected to PFGE, transferred to nitrocellulose membrane, and hybridized with probes of telomere proximal fragments C, I, M, and L. In *taz1*Δ *stn1-226* double mutant, these fragments were absent, suggesting that chromosomes are circular.

Downloaded from http://advances.sciencemag.org/ on November 26, 2020

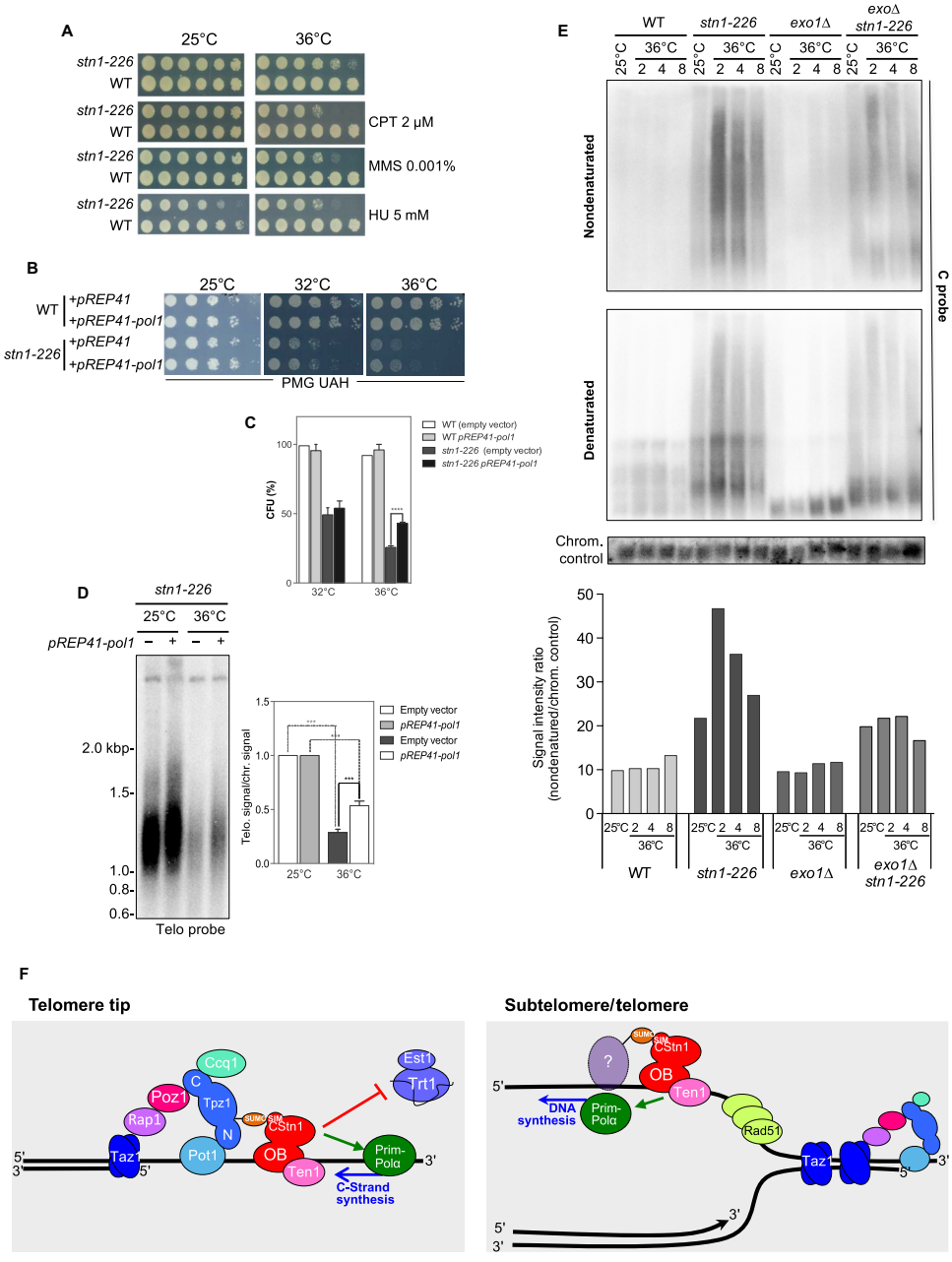

Fig. 6. Stn1-Ten1 promotes DNA synthesis at telomeres to limit ssDNA accumulation. (**A**) WT and *stn1-226* cells were grown at 25°C, then serially diluted (fivefold), and plated on YES-rich medium in the presence of the indicated drugs. (**B**) WT and *stn1-226* cells containing pREP41 (empty vector) or pREP41-Pol1 plasmids were grown at 25°C in selective medium (PMG UAH), then serially diluted (fivefold), and plated. Plates were incubated at 25°, 32°, and 36°C. (**C**) Plating efficiencies were measured for WT and *stn1-226* cells containing pREP41 (empty vector) or pREP41-Pol1 plasmids. Cells were grown at 25°C in selective medium and enumerated, and approximately a thousand cells were plated in triplicate. Plates were incubated at 25°, 32°, and 36°C. The plating efficiency was calculated by determining the ratio of CFU at 32° and 36°C above CFU at 25°C. Error bars indicate the SEM from multiple independent experiments ($n = 4$); P values are calculated from two-tailed t test (****$P < 0.0001$). (**D**) Overexpression of Pol1 partially complements *stn1-226* defects. *stn1-226* strains containing either pREP41 (empty vector) or pREP41-Pol1 were cultivated at 25°C in selective medium (PMG UAH) and then shifted at 36°C for 24 hours. Genomic DNA was prepared, digested with Eco RI restriction enzyme, and analyzed by Southern blotting with radiolabeled telomeric and chromosomic probes. Quantification of telomeric signal over chromosomic signal is presented. Error bars indicate the SEM from multiple independent experiments ($n = 3$); P values are calculated from two-tailed t test (***$P < 0.005$). (**E**) Analysis of Nsi I–digested genomic DNA was performed using in-gel nondenaturing hybridization, using a telomeric C probe. The same gel was denatured and rehybridized with the same probe and then hybridized again with a chromosomic probe (loading control). The G-strand signal intensities were quantified, and the ratio of intensities for nondenatured signal over denatured loading signal was calculated and plotted. (**F**) Dual action of Stn1-Ten1 complex at telomeres. Left: The Stn1-Ten1 complex acts as a modulator of telomerase action through the SIM domain of Stn1 and likely promotes the synthesis of the complementary strand by facilitating Polα action at telomere extremities. Right: At the subtelomeric and telomeric regions, the slowdown of the replication fork may accentuate the accumulation of nascent ssDNA. Thus, accessory factors are required to promote the replications of telomeres. The Stn1-Ten1 complex is likely required to either initiate or facilitate de novo DNA synthesis by the Prim-Polα complex. The interaction of Stn1 with a sumoylated partner through its SIM domain remains hypothetical. Stn1-Ten1 acts in a pathway that is independent of Taz1 and also distinct from Rad51, which might be required to protect nascent ssDNA at stalled fork at telomeres.

Downloaded from http://advances.sciencemag.org/ on November 26, 2020

function of Stn1(-Ten1) contributes to DNA synthesis either for the synthesis of complementary strands or during the replication of telomeric/subtelomeric regions, then one could expect to detect an increase of telomeric ssDNA in *stn1-226* background. Therefore, we performed in-gel nondenaturing hybridization with a C-rich probe to detect telomeric G-strands in Nsi I–digested DNA from WT and *stn1-226* cells collected either at 25°C or after 2, 4, and 8 hours at 36°C. Then, the gel was denatured and rehybridized with the same C-rich probe or the loading control probe (Fig. 6E). The ratio, nondenatured/loading control, reflects the amount of exposed single-stranded G-strand. We observed a substantial increase of G-strand signal compared to WT in *stn1-226* cells at 25°C, which was further increased at 36°C. Furthermore, inactivation of Exo1 significantly limited the accumulation of ssDNA, suggesting that the *stn1-226* allele generates free 5′ DNA ends sensitive to Exo1 resection. Notably, the deletion of the *exo1* gene also suppresses the growth phenotype of *stn1-226* cells (fig. S2B). Overall, this indicates that *stn1-226* cells exhibit higher levels of G-strand overhang compared to WT and likely accumulate telomeric ssDNA during replication.

DISCUSSION

We identified in fission yeast the SIM in the Stn1 protein. When mutated, this motif provokes the elongation of telomeres. This phenotype is caused by the reduced ability of the Stn1-Ten1 complex to bind telomeres and the concomitant increase of telomerase recruitment, thereby indicating that the Stn1 SIM domain contributes to limit telomerase action. In addition, mutations in the SIM domain confer to Stn1 a *ts* phenotype. We demonstrated that at a high temperature, *stn1-226* cells lose telomeric repeats and subtelomeric regions, emphasizing the role of Stn1 in the replication of these regions. It is likely that at a high temperature, changes in the Stn1 structure modify Stn1 interaction with other partners than Ten1 (for example, unsumoylated Tpz1 or as yet to be identified proteins), explaining the dual function of the Stn1-Ten1 complex (Fig. 6F).

The *stn1-226* allele shares common phenotypes with the previously described *stn1-1* mutant (*28*). Both have elongated telomeres, and the loss of subtelomeric/telomeric sequences observed at a restrictive temperature is rescued by *rif1*Δ. Despite these similarities, both alleles behave differently on a number of points. In contrast to Stn1-1, SIM mutations fully abrogate interaction with SUMO and SUMO-Tpz1 that seems to confer to the *stn1-226* allele more severe phenotypes. At a permissive temperature, replication of the telomere is substantially impaired (Fig. 3B) and accumulation of telomeric ssDNA is significantly increased in *stn1-226* cells (Fig. 6E). The absence of Exo1 partially suppresses telomeric ssDNA accumulation and the growth defect exhibited by *stn1-226* cells, whereas Exo1 inactivation has no impact in *stn1-1* cells. Collectively, our results might reveal that recognition of sumoylated partners is critical for Stn1 function in telomere replication and shed light on the mechanism of Stn1 recruitment (Fig. 6F).

Unexpectedly, when the *stn1-226* allele is combined with the $tpz1^{K242R}$ mutant, a nonsumoylatable form of Tpz1, the double mutant exhibits circular chromosomes, a severe phenotype provoked by the rapid loss of telomeres that is inconsistent with an epistatic relationship between the two mutations. Although it was unexpected, this observation unveils a tightly regulated control of Stn1-Ten1 recruitment at a telomere that is mediated by SUMOylation of Tpz1, the SIM of Stn1, and likely by SUMO-independent interactions between Stn1-Ten1 and Tpz1. This also indicates that the function of the SIM of Stn1 is not limited to the modulation of the interaction between the Stn1 and Tpz1 proteins, which curbs the action of telomerase. Our results suggest that Stn1 is involved via its SIM in the functional interaction with other partner(s), and this interaction is crucial for telomere integrity in the absence of Tpz1 SUMOylation at K242 (Fig. 6F).

Although the requirement of Stn1-Ten1 in the replication of chromosome ends is unambiguous, the mechanism of action of the complex remains unknown. Genetic analysis shows that Stn1-Ten1 likely promotes the progression of replication forks through telomeric regions in synergy with Taz1. The accumulation of G-rich ssDNA and the partial rescue of *stn1-226* phenotype conferred by the overexpression of the catalytic subunit of Polα suggest that Stn1-Ten1 is required to facilitate de novo DNA synthesis by the Prim-Polα complex. This result is also consistent with the growth defect observed in *stn1-226 rad51*Δ cells. An interpretation would be that Rad51 protects nascent ssDNA (*46*) and Stn1 limits its accumulation by promoting DNA synthesis at ssDNA gaps (Fig. 6F). Notably, these observations do not preclude the possibility that Rad51 and Stn1 also act together to limit nascent ssDNA accumulation at stalled replication forks, as it has been described in human cells (*47*). Therefore, one could imagine that Stn1-Ten1 stimulates Polα at chromosome ends in a manner similar to that of RPA in the gap-filling reaction. It has been shown recently in human cells that STN1 alone stimulates the activity of Prim-Polα complex through a direct interaction with POLA2, the regulatory subunit of Polα (*48*). Here, we were unable to show any interaction between the Stn1-Ten1 complex and the different components of the Prim-Polα complex by Y2H. It may that this interaction involves several protein surfaces, explaining our negative Y2H results. How to explain the requirement of Stn1-Ten1 for the replication of subtelomeric and telomeric regions? One possibility is that the poor processivity of the Polα, which may simply fall off while replicating "difficult" sequences, requires accessory factors, such as Stn1-Ten1, to reinitiate the DNA synthesis and Rad51 to protect ssDNA.

One interesting observation is that *stn1-226* defects are fully complemented by the deletion of $rif1^{+}$. Rif1 is a multifaceted protein that is involved in fission yeast in telomerase inhibition, in cytokinesis, and in the timing of the replication at a high temperature (*49*). In budding yeast, ScRif1 also exhibits a DNA repair function as the human RIF1 (*50*, *51*). One possibility is that firing of dormant or cryptic origins in the subtelomeric regions restores the progression of DNA replication into the telomeric regions. Another attractive hypothesis would be that Stn1 is directly involved in promoting the origin firing process, particularly at subtelomeric regions. The involvement of telomerase is less evident, but one could imagine that telomerase processes free DNA ends generated by the collapse of replication forks in telomeric sequences (*52*). One other hypothesis would be that deletion of $rif1^{+}$ promotes the resolution of telomere entanglements that may arise in *stn1-226* cells. In the future, we will address these questions to establish the genetic connections that exist between Stn1 and Rif1 proteins.

Because human CST shares common characteristics with the Stn1-Ten1 fission yeast complex, we asked whether SUMOylation-mediated accumulation of STN1-TEN1 at telomeres might be conserved in humans. We identified several potential motifs in human CSTN1 that resemble SIMs domains, and we used the Y2H approach to monitor CSTN1/SUMO1-3 interactions. We failed to detect these interactions, suggesting that SUMOylation-dependent recruitment of STN1-TEN1 might not be a conserved feature in humans. We can hypothesize that *S. pombe* cells could eventually compensate the absence of CTC1 by the Tpz1-SUMO/SIM-Stn1 interaction. Collectively, our results demonstrate

Downloaded from http://advances.sciencemag.org/ on November 26, 2020

that Stn1-Ten1 in fission yeast shares two common functions with human CST: It limits telomerase activity and plays an important role in telomere replication (Fig. 6F). This raises the question of how Stn1-Ten1 is recruited to subtelomeres and telomeres to fulfill its replication functions. The sensitivity of the *stn1-226* strain to DNA-damaging agents may also suggest that Stn1-Ten1 is required genome-wide perhaps at specific sites to restart stalled forks, as is the CST complex in human cells (*12*). Thus, it is possible that Stn1-Ten1 binds directly to ssDNA or necessitates the presence of a sumoylated partner.

MATERIALS AND METHODS

Strains and plasmids

The fission yeast strains and plasmids used in this study are listed in tables S1 and S2, respectively. To generate the *stn1-226* allele that carries mutations ^{226}ILAL^{229} to ^{226}AAAA^{229}, we cloned a genomic DNA fragment containing the *stn1*$^+$ gene into pJK210 plasmid using primers: ^{546}FwStn1^{XhoI}, 5′-gatcctcgagTTAAAAAATTTTTCTATTGTCAGCAATCG-3′; ^{547}RevStn1^{BamHI}, 5′-gatcggatccCTCATGACTTCCAACTATAATAATC-3′ (*53*). The pJK210-stn1 plasmid was mutagenized to create the pJK210-stn1-226. The Pac I–linearized pJK210-stn1-226 plasmid was transformed into a WT strain, and cells were plated on minimum medium lacking uracil. Ura4$^+$ cells were streaked on 5-fluoroorotic acid plate to force direct-repeat recombination between *stn1*$^+$ and *stn1-226* alleles. *stn1-226* allele was verified by sequencing. C-terminal epitope tagging was performed by one-step homologous insertion (*54*).

Telomere length analysis by Southern blotting

Genomic DNA was prepared and digested by Apa I or Eco RI, separated on 1.2% agarose gel, and then transferred onto a Hybond-XL membrane, as previously described (*36*). After transfer, the membrane was hybridized with radiolabeled telomeric and subtelomeric (STE1) probes (*55*). A chromosomic probe was also used as a loading control. It corresponded to a genomic region of chromosome II that could be amplified by the following primers: 679, 5′-GATTTCGGGGTCCAGGAAAC-3′; 680, 5′-CTGTTCGTAATCGAAGATGGG-3′. This probe revealed a 2.4-kbp fragment when genomic DNA was digested with Apa I.

Chromatin immunoprecipitation

ChIPs were performed as previously described (*36*). 9E10 anti-myc (Santa Cruz Biotechnology), M2 anti-Flag (Sigma-Aldrich), and anti-V5 (Invitrogen) mouse monoclonal antibodies were used. Input and immunoprecipitated DNAs were spotted onto a Hybond-XL membrane before hybridization with a radiolabeled telomeric probe. Values corresponded to the immunoprecipitated signal normalized to input signal.

Y2H assay

Yeast strains were derived from EGY48 (*MATα*, *ura3*, *his3*, *trp1*, and *LexA*$_{op(x6)}$*-LEU2*) containing the pSH18-34 (*LexA*$_{op(x8)}$*-LacZ*, *URA3*, and *amp*^{r}) plasmid. The fission yeast complementary DNA (cDNA) of interest was cloned into the pJG4-5 (*B42-AD*, *TRP1*, and *amp*^{r}) and the pEG202 [*LexA*$_{(1–202)}$*DNA-BD*, *HIS3*, and *amp*^{r}] and cotransformed into EGY48 + pSH18-34 strain and plated onto -URA-TRP-HIS medium. To monitor protein interaction, clones were spotted onto 3% Gal-URA-TRP-HIS-LEU and 3% Gal-URA-TRP-HIS-Xgal (80 μg/ml) plates. Plates were incubated at 30°C for 2 to 4 days. For β-galactosidase enzyme measurement, the equivalent of 2 U of OD_{600} (optical density at 600 nm) of cell suspension grown in 3% Gal-URA-TRP-HIS were collected, washed once, and suspended in 800 μl of Z-buffer (pH 7.5; 10 mM KCl, 1 mM $MgSO_4$, 50 mM 2-mercaptoethanol, and 100 mM sodium phosphate). Then, 30 μl of chloroform and 20 μl 0.1% SDS were added. Four hundred microliters of *o*-nitrophenyl-β-D-galactopyranoside (4 mg/ml in Z-buffer) was added, and incubation was continued at 30°C until a detectable yellow color was formed. The reaction was terminated by the addition of 500 μl of 1 M Na_2CO_3, and absorbance at 420 nm was measured. One unit of β-galactosidase is defined as the amount that hydrolyzes 1 μmol of *o*-nitrophenyl-β-D-galactopyranoside to *o*-nitrophenol and D-galactose per minute per cell.

Pulse-field gel electrophoresis

PFGE was performed as previously described (*56*).

2D-gel electrophoresis

2D-gel electrophoresis was performed as described by Noguchi *et al.* (*57*). For the analysis of telomeres, 10 μg of DNA was digested with 60 U of Nsi I. For the analysis of the RFB region, 5 μg of DNA was digested with 60 U of Bam HI. Precipitated DNA was run on 0.4% agarose gel for the first dimension and on 1% agarose gel for the second dimension. Gels were transferred to Hybond-XL membranes, which were probed with the STE1 probe or the 1.35-kbp Eco RI–Eco RI rDNA fragment.

In-gel hybridization

In-gel hybridization was performed as previously described (*58*) by using a G-rich probe (675, 5′-GATCGGGTTACAAGGTTACGTGGTTACACG-3′) and a C-rich probe (676, 5′-CGTGTAACCACGTAACCTTGTAACCCGATC-3′). A chromosomic probe was also used as a loading control. It corresponded to a genomic region of chromosome II that could be amplified by the following primers: 761, 5′-TAGGATGAAAGGAAGAACCG-3′; 762: 5′-GTACTTTACCGGATCATCTCTC-3′. This probe revealed a 1.1-kbp fragment when genomic DNA was digested with Nsi I.

SUPPLEMENTARY MATERIALS

Supplementary material for this article is available at http://advances.sciencemag.org/cgi/content/full/4/5/eaar2740/DC1

table S1. Fission yeast strains used in this study.

table S2. Plasmids used in this study.

fig. S1. Comparison of Stn1-226 with other Stn1 mutants.

fig. S2. Deletion of *rif1*$^+$ and *exo1*$^+$ restores viability of *stn1-226* allele.

REFERENCES AND NOTES

1. W. Palm, T. de Lange, How shelterin protects mammalian telomeres. *Annu. Rev. Genet.* **42**, 301–334 (2008).
2. E. Gilson, V. Géli, How telomeres are replicated. *Nat. Rev. Mol. Cell Biol.* **8**, 825–838 (2007).
3. R. E. Verdun, J. Karlseder, Replication and protection of telomeres. *Nature* **447**, 924–931 (2007).
4. J. C. Schmidt, A. B. Dalby, T. R. Cech, Identification of human TERT elements necessary for telomerase recruitment to telomeres. *eLife* **3**, e03563 (2014).
5. J. Nandakumar, C. F. Bell, I. Weidenfeld, A. J. Zaug, L. A. Leinwand, T. R. Cech, The TEL patch of telomere protein TPP1 mediates telomerase recruitment and processivity. *Nature* **492**, 285–289 (2012).
6. F. L. Zhong, L. Batista, A. Freund, M. F. Pech, A. S Venteicher, S. E. Artandi, TPP1 OB-fold domain controls telomere maintenance by recruiting telomerase to chromosome ends. *Cell* **150**, 481–494 (2012).
7. Y. Miyake, M. Nakamura, A. Nabetani, S. Shimamura, M. Tamura, S. Yonehara, M. Saito, F. Ishikawa, RPA-like mammalian Ctc1-Stn1-Ten1 complex binds to single-stranded

Downloaded from http://advances.sciencemag.org/ on November 26, 2020

DNA and protects telomeres independently of the Pot1 pathway. *Mol. Cell* **36**, 193–206 (2009).
8. L.-Y. Chen, S. Redon, J. Lingner, The human CST complex is a terminator of telomerase activity. *Nature* **488**, 540–544 (2012).
9. D. E. Casteel, S. Zhuang, Y. Zeng, F. W. Perrino, G. R. Boss, M. Goulian, R. B. Pilz, A DNA polymerase-α-primase cofactor with homology to replication protein A-32 regulates DNA replication in mammalian cells. *J. Biol. Chem.* **284**, 5807–5818 (2008).
10. F. Wang, J. A. Stewart, C. Kasbek, Y. Zhao, W. E. Wright, C. M. Price, Human CST has independent functions during telomere duplex replication and C-Strand Fill-In. *Cell Rep.* **2**, 1096–1103 (2012).
11. P. Gu, J.-N. Min, Y. Wang, C. Huang, T. Peng, W. Chai, S. Chang, CTC1 deletion results in defective telomere replication, leading to catastrophic telomere loss and stem cell exhaustion. *EMBO J.* **31**, 2309–2321 (2012).
12. J. A. Stewart, F. Wang, M. F. Chaiken, C. Kasbek, P. D. Chastain, W. E. Wright, C. M. Price, Human CST promotes telomere duplex replication and general replication restart after fork stalling. *EMBO J.* **31**, 3537–3549 (2012).
13. A. Bhattacharjee, J. Stewart, M. Chaiken, C. M. Price, STN1 OB fold mutation alters DNA binding and affects selective aspects of CST function. *PLOS Genet.* **12**, e1006342 (2016).
14. T. Miyoshi, J. Kanoh, M. Saito, F. Ishikawa, Fission yeast Pot1-Tpp1 protects telomeres and regulates telomere length. *Science* **320**, 1341–1344 (2008).
15. B. A. Moser, T. M. Nakamura, Protection and replication of telomeres in fission yeast. *Biochem. Cell Biol.* **87**, 747–758 (2009).
16. P.-M. Dehé, J. P. Cooper, Fission yeast telomeres forecast the end of the crisis. *FEBS Lett.* **584**, 3725–3733 (2010).
17. K. M. Miller, M. G. Ferreira, J. P. Cooper, Taz1, Rap1 and Rif1 act both interdependently and independently to maintain telomeres. *EMBO J.* **24**, 3128–3135 (2005).
18. K. M. Miller, O. Rog, J. P. Cooper, Semi-conservative DNA replication through telomeres requires Taz1. *Nature* **440**, 824–828 (2006).
19. K. Tomita, J. P. Cooper, Fission yeast Ccq1 is telomerase recruiter and local checkpoint controller. *Genes Dev.* **22**, 3461–3474 (2008).
20. B. A. Moser, Y.-T. Chang, J. Kosti, T. M. Nakamura, Tel1^{ATM} and Rad3^{ATR} kinases promote Ccq1-Est1 interaction to maintain telomeres in fission yeast. *Nat. Struct. Mol. Biol.* **18**, 1408–1413 (2011).
21. H. Yamazaki, Y. Tarumoto, F. Ishikawa, Tel1^{ATM} and Rad3^{ATR} phosphorylate the telomere protein Ccq1 to recruit telomerase and elongate telomeres in fission yeast. *Genes Dev.* **26**, 241–246 (2012).
22. K. Miyagawa, R. S. Low, V. Santosa, H. Tsuji, B. A. Moser, S. Fujisawa, J. L. Harland, O. N. Raguimova, A. Go, M. Ueno, A. Matsuyama, M. Yoshida, T. M. Nakamura, K. Tanaka, SUMOylation regulates telomere length by targeting the shelterin subunit Tpz1^{Tpp1} to modulate shelterin–Stn1 interaction in fission yeast. *Proc. Natl. Acad. Sci. U.S.A.* **111**, 5950–5955 (2014).
23. M. Garg, R. L. Gurung, S. Mansoubi, J. O. Ahmed, A. Davé, F. Z. Watts, A. Bianchi, Tpz1^{TPP1} SUMOylation reveals evolutionary conservation of SUMO-dependent Stn1 telomere association. *EMBO Rep.* **15**, 871–877 (2014).
24. Y.-T. Chang, B. A. Moser, T. M. Nakamura, Fission yeast shelterin regulates DNA polymerases and Rad3^{ATR} kinase to limit telomere extension. *PLOS Genet.* **9**, e1003936 (2013).
25. V. Martin, L.-L. Du, S. Rozenzhak, P. Russell, Protection of telomeres by a conserved Stn1–Ten1 complex. *Proc. Natl. Acad. Sci. U.S.A.* **104**, 14038–14043 (2007).
26. J. Sun, E. Y. Yu, Y. Yang, L. A. Confer, S. H. Sun, K. Wan, N. F. Lue, M. Lei, Stn1–Ten1 is an Rpa2–Rpa3-like complex at telomeres. *Genes Dev.* **23**, 2900–2914 (2009).
27. L. Aravind, V. Anantharaman, S. Balaji, M. M. Babu, L. M. Iyer, The many faces of the helix-turn-helix domain: Transcription regulation and beyond. *FEMS Microbiol. Rev.* **29**, 231–262 (2005).
28. M. Takikawa, Y. Tarumoto, F. Ishikawa, Fission yeast Stn1 is crucial for semi-conservative replication at telomeres and subtelomeres. *Nucleic Acids Res.* **45**, 1255–1269 (2017).
29. B. Xhemalce, E. M. Riising, P. Baumann, A. Dejean, B. Arcangioli, J.-S. Seeler, Role of SUMO in the dynamics of telomere maintenance in fission yeast. *Proc. Natl. Acad. Sci. U.S.A.*. **104**, 893–898 (2007).
30. B. Xhemalce, J.-S. Seeler, G. Thon, A. Dejean, B. Arcangioli, Role of the fission yeast SUMO E3 ligase Pli1p in centromere and telomere maintenance. *EMBO J.* **23**, 3844–3853 (2004).
31. J. Song, L. K. Durrin, T. A. Wilkinson, T. G. Krontiris, Y. Chen, Identification of a SUMO-binding motif that recognizes SUMO-modified proteins. *Proc. Natl. Acad. Sci. U.S.A.*. **101**, 14373–14378 (2004).
32. J. T. Hannich, A. Lewis, M. B. Kroetz, S.-J. Li, H. Heide, A. Emili, M. Hochstrasser, Defining the SUMO-modified proteome by multiple approaches in *Saccharomyces cerevisiae*. *J. Biol. Chem.* **280**, 4102–4110 (2005).
33. C.-M. Hecker, M. Rabiller, K. Haglund, P. Bayer, I. Dikic, Specification of SUMO1- and SUMO2-interacting motifs. *J. Biol. Chem.* **281**, 16117–16127 (2006).
34. T. Naito, A. Matsuura, F. Ishikawa, Circular chromosome formation in a fission yeast mutant defective in two ATM homologues. *Nat. Genet.* **20**, 203–206 (1998).
35. T. M. Nakamura, J. P. Cooper, T. R. Cech, Two modes of survival of fission yeast without telomerase. *Science* **282**, 493–496 (1998).
36. J. Audry, L. Maestroni, E. Delagoutte, T. Gauthier, T. M. Nakamura, Y. Gachet, C. Saintomé, V. Géli, S. Coulon, RPA prevents G-rich structure formation at lagging-strand telomeres to allow maintenance of chromosome ends. *EMBO J.* **34**, 1942–1958 (2015).
37. A. Sánchez-Gorostiaga, C. López-Estraño, D. B. Krimer, J. B. Schvartzman, P. Hernández, Transcription termination factor reb1p causes two replication fork barriers at its cognate sites in fission yeast ribosomal DNA in vivo. *Mol. Cell. Biol.* **24**, 398–406 (2004).
38. S. Coulon, E. Noguchi, C. Noguchi, L.-L. Du, T. M. Nakamura, P. Russell, Rad22^{Rad52}-dependent repair of ribosomal DNA repeats cleaved by Slx1-Slx4 endonuclease. *Mol. Biol. Cell* **17**, 2081–2090 (2006).
39. L. Maestroni, S. Matmati, S. Coulon, Solving the telomere replication problem. *Genes (Basel)*. **8**, 55 (2017).
40. M. Hayano, Y. Kanoh, S. Matsumoto, C. Renard-Guillet, K. Shirahige, H. Masai, Rif1 is a global regulator of timing of replication origin firing in fission yeast. *Genes Dev.* **26**, 137–150 (2012).
41. Y. Kanoh, S. Matsumoto, R. Fukatsu, N. Kakusho, N. Kono, C. Renard-Guillet, K. Masuda, K. Iida, K. Nagasawa, K. Shirahige, H. Masai, Rif1 binds to G quadruplexes and suppresses replication over long distances. *Nat. Struct. Mol. Biol.* **22**, 889–897 (2015).
42. D. Jain, A. K. Hebden, T. M. Nakamura, K. M. Miller, J. P. Cooper, HAATI survivors replace canonical telomeres with blocks of generic heterochromatin. *Nature* **467**, 223–227 (2010).
43. J. Kanoh, F. Ishikawa, spRap1 and spRif1, recruited to telomeres by Taz1, are essential for telomere function in fission yeast. *Curr. Biol.* **11**, 1624–1630 (2001).
44. S. Zaaijer, N. Shaikh, R. K. Nageshan, J. P. Cooper, Rif1 regulates the fate of DNA entanglements during mitosis. *Cell Rep.* **16**, 148–160 (2016).
45. A. Davé, C. Cooley, M. Garg, A. Bianchi, Protein phosphatase 1 recruitment by Rif1 regulates DNA replication origin firing by counteracting DDK activity. *Cell Rep.* **7**, 53–61 (2014).
46. Y. Hashimoto, A. R. Chaudhuri, M. Lopes, V. Costanzo, Rad51 protects nascent DNA from Mre11-dependent degradation and promotes continuous DNA synthesis. *Nat. Struct. Mol. Biol.* **17**, 1305–1311 (2010).
47. M. Chastain, Q. Zhou, O. Shiva, L. Whitmore, P. Jia, X. Dai, C. Huang, M. Fadri-Moskwik, P. Ye, W. Chai, Human CST facilitates genome-wide RAD51 recruitment to GC-rich repetitive sequences in response to replication stress. *Cell Rep.* **16**, 1300–1314 (2016).
48. S. Ganduri, N. F. Lue, STN1–POLA2 interaction provides a basis for primase-pol α stimulation by human STN1. *Nucleic Acids Res.* **45**, 9455–9466 (2017).
49. H. Masai, Y. Kanoh, K. Moriyama, S. Yamazaki, N. Yoshizawa, S. Matsumoto, Telomere-binding factors in the regulation of DNA replication. *Genes Genet. Syst.* **92**, 119–125 (2018).
50. C. Ribeyre, D. Shore, Anticheckpoint pathways at telomeres in yeast. *Nat. Struct. Mol. Biol.* **19**, 307–313 (2012).
51. S. Mattarocci, J. K. Reinert, R. D. Bunker, G. A. Fontana, T. Shi, D. Klein, S. Cavadini, M. Faty, M. Shyian, L. Hafner, D. Shore, N. H. Thomä, U. Rass, Rif1 maintains telomeres and mediates DNA repair by encasing DNA ends. *Nat. Struct. Mol. Biol.* **24**, 588–595 (2017).
52. M.-N. Simon, D. Churikov, V. Géli, Replication stress as a source of telomere recombination during replicative senescence in *Saccharomyces cerevisiae*. *FEMS Yeast Res.* **16**, fow085 (2016).
53. J. B. Keeney, J. D. Boeke, Efficient targeted integration at leu1-32 and ura4-294 in Schizosaccharomyces pombe. *Genetics* **136**, 849–856 (1994).
54. J. Bähler, J.-Q. Wu, M. S. Longtine, N. G. Shah, A. Mckenzie III, A. B. Steever, A. Wach, P. Philippsen, J. R. Pringle, Heterologous modules for efficient and versatile PCR-based gene targeting in *Schizosaccharomyces pombe*. *Yeast* **14**, 943–951 (1998).
55. O. Rog, K. M. Miller, M. G. Ferreira, J. P. Cooper, Sumoylation of RecQ helicase controls the fate of dysfunctional telomeres. *Mol. Cell* **33**, 559–569 (2009).
56. T. M. Nakamura, B. A. Moser, P. Russell, Telomere binding of checkpoint sensor and DNA repair proteins contributes to maintenance of functional fission yeast telomeres. *Genetics* **161**, 1437–1452 (2002).
57. E. Noguchi, C. Noguchi, L.-L. Du, P. Russell, Swi1 prevents replication fork collapse and controls checkpoint kinase Cds1. *Mol. Cell Biol.* **23**, 7861–7874 (2003).
58. K. Tomita, A. Matsuura, T. Caspari, A. M. Carr, Y. Akamatsu, H. Iwasaki, K.-i. Mizuno, K. Ohta, M. Uritani, T. Ushimaru, K. Yoshinaga, M. Ueno, Competition between the Rad50 complex and the Ku heterodimer reveals a role for Exo1 in processing double-strand breaks but not telomeres. *Mol. Cell Biol.* **23**, 5186–5197 (2003).

Acknowledgments: We thank B. Moser for the Y2H plasmids, J. Lingner for the human *STN1* cDNA, S. Scaglione and P.-M. Dehé for the technical assistance, and J.-H. Guervilly for

Downloaded from http://advances.sciencemag.org/ on November 26, 2020

the SUMO site identification. We also thank D. Churikov and the members of VG team for the helpful discussions. **Funding:** The VG laboratory is supported by the Ligue Nationale Contre le Cancer (LNCC) (Equipe Labéllisée) and by the Agence Nationale de la Recherche (ANR-Blanc Quiescence DNA SVSE8). S.C. is supported by Projet Fondation ARC. S.M. is supported by the LNCC and L.M. is supported by the ANR-Blanc Quiescence DNA SVSE8. T.M.N. is supported by the NIH grant no. R01GM078253. M.G.F and J.M.E are supported by Portuguese Fundação para a Ciência e a Tecnologia grant PTDC/BEX-BCM/5179/14. **Author contributions:** S.M., M.V., J.M.E., L.M., and S.C. designed and performed the experiments and analyzed the data. J.M.E., M.G.F., T.M.N., V.G., and S.C. discussed the data. S.C. and V.G. wrote the manuscript. **Competing interests:** All authors declare that they have no competing interests. **Data and materials availability:** All data needed to evaluate the conclusions in the paper are present in the paper and/or the Supplementary Materials. Additional data related to this paper may be requested from the authors.

Submitted 20 October 2017
Accepted 29 March 2018
Published 16 May 2018
10.1126/sciadv.aar2740

Citation: S. Matmati, M. Vaurs, J. M. Escandell, L. Maestroni, T. M. Nakamura, M. G. Ferreira, V. Géli, S. Coulon, The fission yeast Stn1-Ten1 complex limits telomerase activity via its SUMO-interacting motif and promotes telomeres replication. *Sci. Adv.* **4**, eaar2740 (2018).

Downloaded from http://advances.sciencemag.org/ on November 26, 2020

ScienceAdvances

The fission yeast Stn1-Ten1 complex limits telomerase activity via its SUMO-interacting motif and promotes telomeres replication

Samah Matmati, Mélina Vaurs, José M. Escandell, Laetitia Maestroni, Toru M. Nakamura, Miguel G. Ferreira, Vincent Géli and Stéphane Coulon

Sci Adv **4** (5), eaar2740.
DOI: 10.1126/sciadv.aar2740

ARTICLE TOOLS http://advances.sciencemag.org/content/4/5/eaar2740

SUPPLEMENTARY MATERIALS http://advances.sciencemag.org/content/suppl/2018/05/14/4.5.eaar2740.DC1

REFERENCES This article cites 58 articles, 24 of which you can access for free
http://advances.sciencemag.org/content/4/5/eaar2740#BIBL

PERMISSIONS http://www.sciencemag.org/help/reprints-and-permissions

Use of this article is subject to the Terms of Service

Science Advances (ISSN 2375-2548) is published by the American Association for the Advancement of Science, 1200 New York Avenue NW, Washington, DC 20005. The title *Science Advances* is a registered trademark of AAAS.

Copyright © 2018 The Authors, some rights reserved; exclusive licensee American Association for the Advancement of Science. No claim to original U.S. Government Works. Distributed under a Creative Commons Attribution NonCommercial License 4.0 (CC BY-NC).

Downloaded from http://advances.sciencemag.org/ on November 26, 2020